Journal of Alloys and Compounds 502 (2010) L14–L16

Contents lists available at ScienceDirect

Journal of Alloys and Compounds

journal homepage: www.elsevier.com/locate/jallcom

Letter

Thermal evaporation route to zinc stannate nanowires and the cathodoluminescence of the individual nanowires

Yinxiao Du*, Pei Ding

Department of Mathematics and Physics, Zhengzhou Institute of Aeronautical Industry Management, Zhengzhou 450015, P.R. China

ARTICLE INFO

Article history:
Received 7 March 2010
Received in revised form 27 March 2010
Accepted 2 April 2010
Available online 24 April 2010

Keywords:
Nanostructured materials
Semiconductors
Gas–solid reactions
Optical property

ABSTRACT

A facile thermal evaporation method was developed to synthesize face-centered cubic spinel zinc stannate (Zn_2SnO_4) nanowires at high temperature. The Zn_2SnO_4 nanowires are well crystalline and the average length is about 10 μm. It is found that the growth process follows Au-catalytic vapor–liquid–solid (VLS) mechanism. The cathodoluminescence (CL) spectra of individual nanowires reveal unusual red emission band centered at 637 and 710 nm, respectively. The excess Zn^{2+} is the main reason for the emission band centered at 637 nm, and the other red emission at 710 nm probably originates from the typical point defects.

© 2010 Elsevier B.V. All rights reserved.

1. Introduction

Transparent conducting oxides (TCO) are certain to be required for various important optical and electric applications due to their interesting cubic spinel structure (AB_2O_4) [1–5]. As one of the most important TCO semiconductors with wide band gap of 3.6 eV, zinc stannate (Zn_2SnO_4) has been considered as promising materials as chemical sensors, TC electrodes and photocatalysts due to its high chemical sensitivity, low visible absorption and low electrical conductivity [6–11]. Recently, Zn_2SnO_4 nanowires have attracted considerable attentions due to their potential scientific studies and applications in optoelectronics and photocatalysis [12,13]. Up to now, the generally chemical vapor deposition (CVD) based methods have been developed to synthesize the Zn_2SnO_4 nanowires. Vapor–liquid–solid (VLS) assisted by Au catalysts and direct vapor–solid (VS) processes were employed to fabricate the nanowires using ZnO/Zn and SnO_2/SnO as source materials [14–17]. Nevertheless, as a well-known synthesis route to various kinds of nanowires, direct thermal evaporation has not reported up to now. In this paper, we reported a facile thermal evaporation route to well crystalline Zn_2SnO_4 nanowires assisted with Au catalysts. The structural properties and growth mechanism were investigated. Moreover, cathodoluminescence (CL) properties of individual nanowires are also measured and presented some interesting features.

2. Experimental

The Zn_2SnO_4 nanowires were fabricated by a facile thermal evaporation method using Zn_2SnO_4 powders as source materials. In the experiment, Zn_2SnO_4 powders were placed in an alumina boat loaded inside the center of alumina tube reactor. Si substrates coated with 1 mM $HAuCl_4{\cdot}3H_2O$ ethanol solution was positioned at a distance of 20 cm from the alumina boat. Ar with flow rate of 200 sccm was introduced in the whole experiment process. The furnace temperature was set to 1700 °C and held at the peak temperature for an hour. Finally, the temperature was cooled down to room temperature and white precipitates were found to deposit on the Si substrates. The crystal structure of the products was analyzed by X-ray diffraction (XRD, Rigaku, Cu Kα radiation, λ = 1.5418 Å at 40 kV and 160 mA). The morphology, microstructures and chemical composition of the products were characterized by field emission scanning electron microscopy (FE-SEM; FEI XL30 S-FEG), and transmission electron microscope equipped with energy-dispersive X-ray spectroscopy (TEM; Philips CM200), respectively. The diffraction peaks were indexed according to the standard diffraction data shown in the software PCPDFWIN (http://icdd.com/products/pdf2.htm). The lattice constants were calculated by using the computer software Divol. The CL studies of individual nanowires were performed in the scanning electron microscope equipped with an Oxford Instruments MonoCL2 spectrometer. For the CL measurement, the accelerating voltage and probe current were 20 kV and 300 pA, respectively.

3. Results and discussion

The morphology of the as-deposited product is shown in Fig. 1. There are large amount of wire-like products with average length of 10 μm grown on the Si substrates (Fig. 1a). These nanowires are straight along growth direction (Fig. 1b), while the surface is not smooth, which is due to instability of atmosphere in the furnace. The composition of the nanowires was measured by EDS, as shown in Fig. 2a. The nanowires are mainly consisted of Zn, Sn and O elements. The detected Si signal came from the Si substrates and is

* Corresponding author. Tel.: +86 371 68252171; fax: +86 371 68252171.
E-mail address: dyxiphy@yahoo.cn (Y. Du).

0925-8388/$ – see front matter © 2010 Elsevier B.V. All rights reserved.
doi:10.1016/j.jallcom.2010.04.121

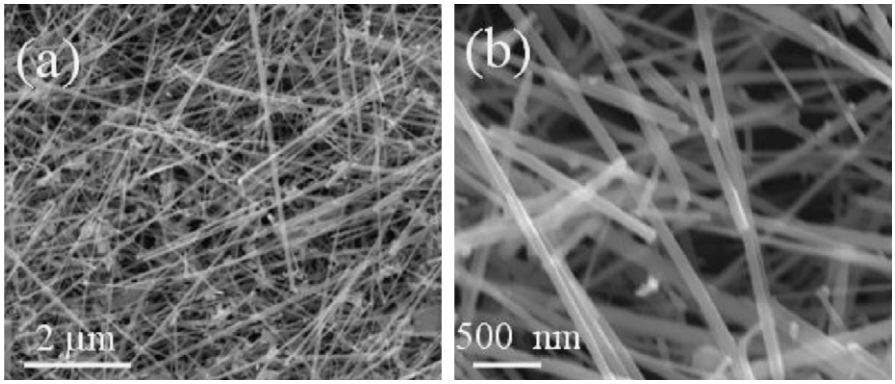

Fig. 1. (a and b) SEM and enlarged SEM image of the nanowires, respectively.

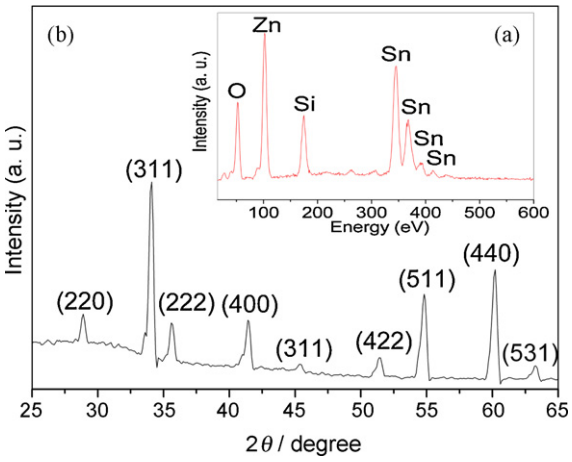

Fig. 2. (a) EDS spectrum of the nanowires. (b) XRD pattern of the nanowires.

not related to the composition of the nanowires. Fig. 2b presents the XRD patterns of the as-synthesized nanowires. The diffraction peaks of (2 2 0), (3 1 1), (2 2 2), (4 0 0), (3 3 1), (4 2 2), (5 1 1), (4 4 0) and (5 3 1) reflections can be indexed as face-centered cubic spinel Zn_2SnO_4 with constants of $a = 8.643(6)$ Å, agreeing well with the calculated diffraction pattern (ICDD-PDF No. 24-1470). Combined the XRD and EDS results, the nanowires are Zn_2SnO_4 nanowires with face-centered cubic spinel structure.

Fig. 3a shows typical image of an individual Zn_2SnO_4 nanowire. The diameter and length of the nanowire are ca. 100 nm and 10 μm, respectively. A nanoparticle is observed to attach on the tip of the nanowire. The nanoparticles are confirmed as metal Au, indicating the typical Au-catalytic VLS growth process. The corresponding TEM-based EDS spectrum (Fig. 3b) exhibits that the nanowire is composed of O, Zn and Sn elements. The ratio of Zn/Sn is about 2.181:1, indicating the excess Zn in the formation of Zn_2SnO_4. As shown in Fig. 3c, the HRTEM image of the Zn_2SnO_4 nanowires clearly indicates that spacing distance of two adjacent fringes is 0.305 nm, matching well with that of (2 2 0) planes of face-centered cubic Zn_2SnO_4 (ICDD-PDF No. 24-1470). No obvious bulk defects such as stacking faults and dislocations can be observed in the crystal lattice, indicating the perfect single-crystal nature of the nanowire. Combined with the HRTEM image and Fast Fourier transformation (FFT) pattern, the growth direction is determined to grow along [1 1 1].

We also conduct the experiment without Au catalyst. No products were detected to deposit on the Si substrates, revealing that Au catalyst plays an important role in the growth of the Zn_2SnO_4 nanowires. It can be clearly seen from the TEM image (Fig. 3a) that the growth mechanism follows typical Au-catalytic VLS process. We deduce that the growth of the nanowires involves a three-step process: Zn_2SnO_4 source materials first decompose into Zn, ZnO_x and SnO_2 vapor at high temperatures. Then, the melting Au liquid drop continuously absorb Zn, ZnO_x and SnO_2 vapor to further form Zn_2SnO_4 droplet. When the supersaturation of Zn_2SnO_4 is up to critical value, the Zn_2SnO_4 droplet will be deposited into solid nuclei. Finally, the growth process will continuously occur, resulting in the formation of Zn_2SnO_4 nanowires.

Fig. 4 presents the room temperature CL spectra of individual Zn_2SnO_4 nanowires. Here we measure CL spectra of four nanowires that are denoted by (a), (b), (c) and (d) in Fig. 4. The spectra have been normalized for comparing the difference in position of emis-

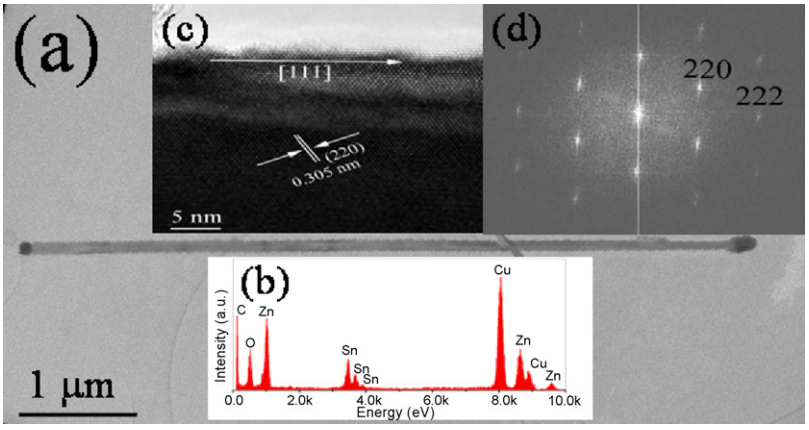

Fig. 3. (a) TEM image of an individual nanowire. (b) TEM-based EDS spectrum of the nanowires. (c) HRTEM image of the nanowire. (d) FFT pattern of the nanowire.

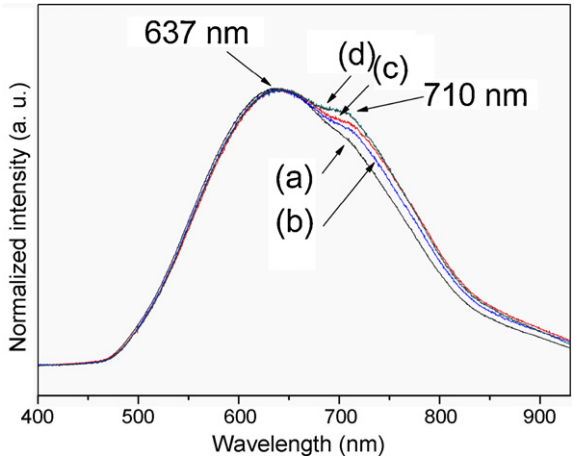

Fig. 4. (a–d) CL spectra taken from the different individual Zn_2SnO_4 nanowires, respectively.

sion peaks of these four spectra. As shown in Fig. 4, four CL spectra exhibit similar emission characteristics: strong and broad red emission band centered at 637 and 710 nm, respectively, which is not been reported before. The exact CL mechanism is rather complicated. Various emission bands e.g. green emission, yellow emission, and red emission had been reported [13,16–18]. It is concluded that the emission properties of Zn_2SnO_4 nanowires are very sensitive to that Zn/Sn stoichiometry and point defects. It is demonstrated from the EDS result (Fig. 3b) that Zn is relatively excess in the Zn_2SnO_4 nanowires. As is known, Zn_2SnO_4 belongs to the group of "4-2" cubic oxide spinels with general formula AB_2O_4 [19,20]. Zn_2SnO_4 is stable in the inverse spinel structure with a face-centered cubic unit cell. Zn^{2+} (B) ions occupy tetrahedral voids and Zn^{2+} (B) and Sn^{4+} (A) ions randomly occupy tetrahedral voids [21]. If Zn^{2+} ions are in excess, the excess Zn^{2+} located at Sn^{4+} site in the spinel structure surrounded by six O^{2-} to form the distorted octahedral structure [22]. The interactions of p orbitals in Zn^{2+} with the orbitals of the six O^{2-} in the distorted octahedral structure will lead to the splitting of new orbitals [23]. It is firmly believed that the emission band centered at 637 nm is attributed to the radiative transition from new energy levels resulting from the distorted octahedral structure. The origin of emission band centered at 710 nm is unknown. Some other factors such as vacancies (V_{Sn}, V_{Zn}, V_O) and intestinal (Zn_i, O_i) may be the main reasons for the unique 710 nm emission band. The exact mechanism needs to be further investigated in detail.

4. Conclusions

In summary, single crystalline Zn_2SnO_4 nanowires with cubic spinel structure were synthesized via a facile thermal evaporation method assisted by Au catalysts. The Zn_2SnO_4 nanowires were well crystalline and were straight along growth direction. It is found that the growth mechanism follows a typical VLS process. The CL spectra of individual nanowires indicate unusual red emission bands centered at 637 and 710 nm, respectively. It is thought that excess Zn^{2+} is the main reason for the emission band centered at 637 nm. The excess Zn^{2+} located at Sn^{4+} sites in the inverse spinel structure surrounded by six O^{2-} to form the distorted octahedral structure, which leads to the radiative transition from new energy levels. The other unusual red emission band at 710 nm probably originates from the typical point defects.

Acknowledgements

This work was financially supported by the Natural Science Foundation of Henan Provincial Educational Department (No. 2010B140015), the Aeronautical Science Foundation of China (No. 2008ZF55006) and the Key Project Foundation of Science and Technology of Henan Province (No. 092102210166).

References

[1] T.J. Coutts, D.L. Young, X. Li, W.P. Mulligan, X. Wu, J. Vac. Sci. Technol. A 18 (2000) 2646–2660.
[2] M. Lei, Q.R. Hu, X. Wang, S.L. Wang, W.H. Tang, J. Alloys Compd. 489 (2010) 663–666.
[3] I.A. Rauf, J. Yuan, Mater. Lett. 5 (1995) 217–220.
[4] M.H. Cao, I. Djerdj, M. Antonietti, M. Niederberger, Chem. Mater. 19 (2007) 5830–5832.
[5] M. Lei, Q.R. Hu, S.L. Wang, W.H. Tang, Mater. Lett. 63 (2009) 1928– 1930.
[6] G. Fu, H. Chen, Z.X. Chen, J.X. Zhang, H. Kohler, Sens. Actuators 81 (2002) 308–312.
[7] F. Belliard, P.A. Connor, J.T.S. Irvine, Solid State Ionics 135 (2000) 163–167.
[8] W.B. Jackon, R.L. Hoffman, G.S. Herman, Appl. Phys. Lett. 87 (2005) 193503.
[9] K. Satoh, Y. Kakehi, A. Okamoto, S. Murakami, Jpn. J. Appl. Phys. 44 (2005) L34–L37.
[11] W.W. Wang, Y.J. Zhu, L.X. Yang, Adv. Funct. Mater. 17 (2007) 59–64.
[12] H.L. Zhu, D.R. Yang, G.X. Yu, H. Zhang, D.L. Jin, K.H. Yao, J Phys. Chem. B 110 (2006) 7631–7634.
[13] J.W. Zhao, L.R. Qin, L.D. Zhang, Solid State Commun. 141 (2007) 663–667.
[14] Y. Li, X.L. Ma, Phys. Status Solidi A 202 (2005) 435–440.
[15] H.S. Kim, S.O. Hwang, Y. Myung, J. Park, Nano Lett. 8 (2008) 551–557.
[16] J.X. Wang, X.W. Sun, S.S. Xie, W.Y. Zhou, Y. Yang, Cryst. Growth Des. 8 (2008) 707–710.
[17] L.S. Wang, X.Z. Zhang, X. Liao, W.G. Yang, Nanotechnology 16 (2005) 2928–2931.
[18] Y. Su, L.A. Zhu, L. Xu, Y.Q. Chen, H.H. Xiao, Q.T. Zhou, Y. Feng, Mater. Lett. 61 (2007) 351–354.
[19] S.H. Wei, S.B. Zhang, Phys. Rev. B 63 (2001) 045112.
[20] M.V. Nikolic, K. Satoh, T. Ivetic, K.M. Paraskevopoulos, T.T. Zorba, V. Blagojevic, L. Mancic, P.M. Nikolic, 516 (2008) 6293–6299.
[21] K.E. Sickafus, J.M. Wills, N.W. Grimes, J. Am. Ceram. Soc. 82 (1999) 3279–3292.
[22] I.J. Hsieh, K.T. Chu, C.F. Yu, J. Appl. Phys. 76 (1994) 3735–3739.
[23] S.S. Yi, I.W. Kim, J.S. Bae, B.K. Moon, S.B. Kim, J.H. Jeong, Mater. Lett. 57 (2002) 904–909.